CrystEngComm

Cite this: *CrystEngComm*, 2011, **13**, 2578

www.rsc.org/crystengcomm

PAPER

Cuprous iodide coordination polymers $(CuI)_x(L)_y \cdot z$(solvent) built on linear thioether linkers†

Jun Zhang, Yun-Shan Xue, Yi-Zhi Li, Hong-Bin Du* and Xiao-Zeng You

Received 30th September 2010, Accepted 23rd December 2010
DOI: 10.1039/c0ce00685h

By using bidentate thioether linkers 1,4-bis(ethylthio)benzene (L_1) and 4,4′-bis(ethylthiomethyl)biphenyl (L_2), four novel coordination polymers $(CuI)_x(L)_y \cdot z$(solvent), MSF–*n* (**m**etal-**s**ulfide-**f**ramework, MSF–6, $x = y = 2$, $L = L_1$; MSF–7, $x = 4$, $y = 2$, $L = L_1$; MSF–8, $x = y = 2$, $L = L_2$; MSF–9, $x = 4$, $y = 1.5$, $L = L_2$) were obtained and characterized by single-crystal X-ray diffraction, thermogravimetric, solid state diffuse reflectance UV-Vis and photoluminescent studies. MSF–*n* ($n = 6$–9) possess 2D layered structures built from $(CuI)_x$ clusters and linear thioether linkers, the formations of which are dependent on the cluster size and linker length. MSF–6 and MSF–8 possess the same structure topology, consisting of lozenge-shaped **sql** single sheets of 4-connecting Cu_2I_2 units and linear thioether linkers L_1 and L_2, respectively. MSF–7 and –9 are cubane cluster Cu_4I_4-based layered compounds, composed of 2-fold interpenetrating **sql** and 3-fold interpenetrating **hcb** sheets, respectively. The solid state diffuse reflectance UV-Vis spectra show that MSF–6 to –9 are wide-gap semiconductors with band gaps of 3.11, 3.25, 3.52 and 3.07 eV, respectively. MSF–7 and –9 are photoluminescent at room temperature owing to the existence of the Cu···Cu interactions within the Cu_4I_4 cluster, while MSF–6 and –8 do not emit upon excitation because of luminescence quenching.

Introduction

Metal–organic coordination polymers have recently attracted great attention because of their potential applications in areas such as absorbent materials, luminescent materials, nonlinear optical (NLO) materials,[1] *etc*. These materials are usually constructed from the combination of metal ions or clusters with multidentate ligands by using a secondary building unit (SBU) approach.[2] Through judicious choice of inorganic building units and organic ligands of a certain coordination geometry, it is possible to prepare novel coordination polymers with specific structures.

To date, many new organic ligands with N- or O-donor atoms,[3] such as carboxylic acids and pyridine derivatives, have been prepared and used as organic SBUs to construct coordination polymers. A few discrete metal clusters of specific coordination geometries as inorganic SBUs to construct coordination polymers have also been reported.[4–6] Among those, the polyhedral clusters of cuprous halides such as Cu_2X_2, Cu_4X_4 (X = halide) have been particularly interesting because these derivatives of Cu(I) are often brightly luminescent even at room temperature.[7] The clusters of copper(I) halides tend to form various coordination networks with nucleophiles such as pyridyl[5,6] and thioether ligands.[8,9] The latter have attracted our attention because of their electron-donor and redox properties, which could result in complexes with potential interesting electrical properties and possible conductivity. Moreover, the coordination chemistry of dithioether ligands has been shown to be rich and diverse as exemplified by numerous aliphatic thioether ligand based copper halide complexes.[9] The formation of these complexes is very dependent on synthetic conditions, ligand lengths or steric/electronic effects exerted by the ligand. In contrast to numerous aliphatic thioether based complexes reported so far, however, the copper halide complexes of aromatic thioether ligands have scarcely been explored. We have been interested in the synthesis of functional coordination polymers by using aromatic S-donor ligands.[10] We used linear thioether linkers 1,4-bis(ethylthio)benzene (L_1) and 4,4′-bis(ethylthiomethyl)biphenyl (L_2) to connect with Cu_xI_x ($x = 2$, 4) clusters (Scheme 1) and obtained a series of coordination polymers $Cu_xI_x(L)_y \cdot z$(solvent), denoted MSF–*n* (**m**etal-**s**ulfide-**f**ramework, $n = 6$–9), respectively. Herein, we report their syntheses, structures, thermogravimetric, solid state UV-Vis diffuse reflectance and photoluminescent properties.

State Key Laboratory of Coordination Chemistry, School of Chemistry and Chemical Engineering, Nanjing University, Nanjing, 210093, China. E-mail: hbdu@nju.edu.cn; Fax: +86-25-83314502; Tel: +86-25-83686581

† Electronic supplementary information (ESI) available: X-Ray crystallographic files (CIF), figures of asymmetric units and PXRD, and tables. CCDC reference numbers 785685–785688. For ESI and crystallographic data in CIF or other electronic format see DOI: 10.1039/c0ce00685h

Experimental section

Materials

All commercially available chemicals are of reagent grade and were used as received without further purification. The ligand

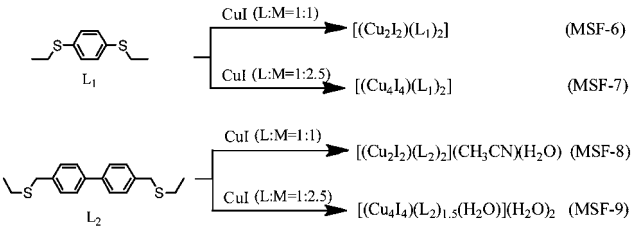

Scheme 1 Synthesis of complexes MSF–6 to 9.

1,4-bis(ethylthio)benzene (L_1) was synthesized according to the literature,[11] and the synthesis of the ligand 4,4′-bis(ethylthiomethyl)biphenyl (L_2) was described in the preparation section.

Physical measurements

Elemental analyses of C, H, and N were performed on an Elementar Vario MICRO Elemental Analyzer at the Analysis Center of Nanjing University. Fourier transformed Infrared (FT-IR) spectra were obtained on a Bruker Vector 22 FT-IR spectrophotometer by using KBr pellets. The solid state diffuse-reflectance UV-Vis spectra were obtained on a Shimadu UV/VIS MPC-3100 Spectrometer. Thermogravimetrical and differential thermal analyses (TG-DTA) were performed in a N_2 atmosphere (a flow rate of 100 ml min^{-1}) on a simultaneous SDT 2960 thermal analyzer from 30 °C up to 800 °C, with a heating rate of 10 °C min^{-1}. X-ray powder diffraction (XRPD) data were collected on a Bruker D8 Advance instrument using a Cu Kα radiation (λ = 1.54056 Å) at room temperature. Solid state photoluminescence spectra were recorded using a SLM48000DSCF/AB2 spectrofluorometer.

Syntheses

Preparation of 4,4′-bis(ethylthiomethyl)biphenyl (L_2). The sodium (0.58 g, 21.2 mmol) was added to the solution of ethanethiol (1.3 ml, 17.6 mmol) in DMF (30 ml) under a nitrogen atmosphere at room temperature. When the sodium disappeared, 4,4′-bis(chloromethyl)biphenyl (1.77 g, 7.04 mmol) was added to the solution in one portion, and the mixture was stirred under nitrogen at 100 °C for about 4 h, then cooled down to room temperature. The mixture was added to 100 ml of water and then extracted with 30 ml of ether 3 times. The organic phase was combined and dried over magnesium sulfate, then the ether was removed to give 1.99 g of products. Yield: 83.1%. ^{1}H NMR (500 MHz, $CDCl_3$): δ: 7.53 (*d*, 4 H), 7.37 (*d*, 4 H), 3.76 (*s*, 4 H), 2.47 (*q*, 4 H), 1.25 (*t*, 6 H).

Synthesis of $(Cu_2I_2)(L_1)_2$ (MSF–6). To the solution of CuI (0.095 g, 0.50 mmol) in 5 ml of acetonitrile was added the solution of L_1 (0.099 g, 0.50 mmol) in 5 ml of acetonitrile to give a clear solution. The solution was placed at room temperature, and the solvent evaporated slowly. After about 6 days, colorless block crystals (0.144 g) were obtained by filtration and washed with acetonitrile three times. Yield: 74.2% (based on L_1). Anal. Calcd for $C_{10}H_{14}CuIS_2$: C, 30.89; H, 3.63%. Found: C, 30.72; H, 3.54%. FT-IR (KBr, cm^{-1}): 3061 w, 2977 m, 2921 m, 2868 m, 1664 w, 1480 s, 1447 s, 1413 s, 1373 s, 1253 s, 1100 w, 1053 m, 1013 m, 966 m, 827 s, 766 s, 640 w, 533 m, 506 s.

Synthesis of $(Cu_4I_4)(L_1)_2$ (MSF–7). To the solution of CuI (0.095 g, 0.50 mmol) in 5 ml of acetonitrile was added the solution of L_1 (0.039 g, 0.20 mmol) in 5 ml of acetonitrile to give a clear solution. The solution was placed at room temperature, and the solvent evaporated slowly. After about 6 days, colorless block crystals (0.071 g) were obtained by filtration and washed with acetonitrile three times. Yield: 61.7% (based on L_1). Anal. Calcd for $C_{60}H_{84}Cu_{12}I_{12}S_{12}$: C, 20.73; H, 2.44%. Found: C, 20.37; H, 2.19%. FT-IR (KBr, cm^{-1}): 3067 w, 2961 m, 2914 m, 2860 m, 1627 w, 1567 w, 1480 s, 1440 s, 1420 s, 1380 s, 1260 s, 1100 w, 1046 m, 1013 s, 966 m, 813 s, 759 m, 660 w, 493 s.

Synthesis of $[(Cu_2I_2)(L_2)_2]\cdot CH_3CN\cdot H_2O$ (MSF–8). To the solution of CuI (0.023 g, 0.12 mmol) in 10 ml of acetonitrile was added the solution of L_2 (0.036 g, 0.12 mmol) in 10 ml of acetonitrile to give a clear solution. The solution was placed at room temperature, and the solvent evaporated slowly. After about 6 days, colorless block crystals (0.050 g) were obtained by filtration and washed with acetonitrile three times. Yield: 84.7% (based on L_2). Anal. Calcd for $C_{76}H_{98}Cu_4I_4N_2O_2S_8$: C, 43.68; H, 4.73; N, 1.34%. Found: C, 43.81; H, 4.61; N, 1.57%. FT-IR (KBr, cm^{-1}): 3027 w, 2972 m, 2921 m, 2868 m, 1920 w, 1607 w, 1496 s, 1453 m, 1413 s, 1393 s, 1373 m, 1253 s, 1106 m, 1040 w, 1006 s, 960 m, 893 s, 813 s, 740 s, 660 w, 533 w, 493 s.

Synthesis of $[(Cu_4I_4)(L_2)_{1.5}(H_2O)]\cdot 2H_2O$ (MSF–9). To the solution of CuI (0.023 g, 0.125 mmol) in 15 ml of acetonitrile was added the solution of L_2 (0.014 g, 0.050 mmol) in 15 ml of acetonitrile to give a clear solution. The solution was placed at room temperature, and the solvent evaporated slowly. After about one month, colorless block crystals (0.021 g) were obtained by filtration and washed with acetonitrile three times. Yield: 50.0% (based on L_2). Anal. Calcd for $C_{27}H_{39}Cu_4I_4O_3S_3$: C, 25.54; H, 3.10%. Found: C, 25.71; H, 3.03%. FT-IR (KBr, cm^{-1}): 3437 m, b, 3024 w, 2964 m, 2923 s, 2870 w, 1913 w, 1606 m, 1494 s, 1447 m, 1417 s, 1395 m, 1385 s, 1261 w, 1233 w, 1146 w, 1110 w, 1000 m, 973 w, 880 w, 822 s, 735 m, 692 w, 630 w, 563 w, 490 w.

X-Ray crystal structure determination

The data collections for single crystal X-ray diffraction for MSF–6 to MSF–9 were carried out on a Bruker Smart APEX II CCD diffractometer at 291 K, using graphite-monochromated Mo-Kα radiation (λ = 0.71073 Å). Data reductions and absorption corrections were performed using the SAINT and SADABS programs,[12] respectively. The structures were solved by direct methods using the SHELXS-97 program and refined with full-matrix least squares on F^2 using the SHELXL-97 program.[13] Anisotropic displacement parameters were refined for all non-hydrogen atoms. The hydrogen atoms were placed in geometrically calculated positions and refined using the riding model.

For MSF–9, the unit cell includes some highly disordered solvent molecules, which could not be modelled as discrete atomic sites. We employed PLATON/SQUEEZE to calculate the diffraction contribution of the solvent molecules and, thereby, to produce a set of solvent-free diffraction intensities.[14] The final density was calculated from the SQUEEZE results, which is the density for the framework. Elemental and TG analyses revealed that the chemical formula of MSF–9 contains two water guest

molecules. Details of the crystal parameters, data collection and refinement results are summarized in Table 1. Selected interatomic bond lengths and angles with their estimated standard deviations are given in Table 2. Detailed interatomic bond lengths and angles for MSF–7 are given in Table S1 (ESI†). Further details can be obtained from the ESI.†

Results and discussion

Synthesis

MSF–*n* (*n* = 6–9) were prepared by the method of solvent evaporation. The phase purity for each compound was confirmed by elemental analyses and X-ray powder diffraction (Fig. S1, ESI†). The formation of MSF–*n* depends on the molar ratio between the ligand and CuI. When the molar ratio between the ligand and CuI was 1 : 1, MSF–6 and MSF–8 with a double-nucleus cluster Cu_2I_2 were obtained. When the ratio was 1 : 2.5, MSF–7 and MSF–9 with a four-nucleus cluster Cu_4I_4 were obtained.

Descriptions of X-Ray crystal structures

Structural analysis of MSF–6. X-ray single crystal diffraction analyses revealed that MSF–6 crystallizes in the centrosymmetric space group *C*2/*m*, which is associated with the point group C_{2h}. The compound is built from a copper–iodine cluster Cu_2I_2 unit and the linear thioether ligand L_1. The asymmetric unit consists of one Cu, one I and a half L_1 ligand (Fig. S2, ESI†). As shown in Fig. 1, the copper atom is in a distorted tetrahedral coordination environment, bonding to two I and two S atoms with the Cu–I length of 2.639(1) Å and Cu–S of 2.340(2) Å, respectively. The interatomic distance between two Cu within the Cu_2I_2 cluster is 2.833(3) Å, slightly larger than the sum of the van der Waals radii (2.80 Å). The bond valence sum calculations[15] for Cu is 1.08, which suggests that Cu is monovalent.

The framework of MSF–6 is constructed from a 4-connecting Cu_2I_2 unit and a linear thioether linker L_1 (Fig. 2). Each linear thioether coordinates *via* its S-donor atoms to two Cu_2I_2 units, while each Cu_2I_2 unit connects with four thioether ligands L_1. This gives rise to a 2D lozenge-shaped sheet of **sql**/Shubnikov topology. The large inner cavities of each lozenge grid with 18.68 × 6.33 Å in diagonal distances are accommodated with four ethyl groups, pointing out of the net plane. The 2D lozenge grid is stacked over each other in an AAA fashion along the c-axis to form a 3D van der Waals network.

Structural analysis of MSF–7. Compound MSF–7 crystallizes in the centrosymmetric space group $P\bar{1}$, which belongs to the point group C_i. The compound is constructed from a copper-iodine cubane cluster Cu_4I_4 unit and the linear thioether ligand L_1 (Fig. 3) The asymmetric unit contains three Cu_4I_4 clusters and six L_1 ligands (Fig. S2, ESI†).

In the cubane-type Cu_4I_4 cluster, each Cu atom adopts a distorted tetrahedral coordination geometry, through bonding to three μ3–I atoms and one S from L_1 ligand. The bond lengths range 2.644(1)–2.753(1) Å for Cu–I and 2.303(2)–2.318(1) Å for Cu–S, consistent with those reported for other respective complexes,[5,6,16] The interatomic lengths of Cu···Cu range from 2.759(1) to 2.880(1) Å, which are similar to those found in other related structures.[6] The bond valence sum calculations[15] for Cu range 0.92–0.99, suggest that Cu is monovalent and there exist significant Cu···Cu interactions in the clusters.

The framework of MSF–7 is constructed from a 4-connecting Cu_4I_4 unit and a linear thioether linker L_1. Similar to that of MSF–6, each linear thioether L_1 in MSF–7 coordinates *via* its S-donor atoms to two Cu_4I_4 units, while each Cu_4I_4 unit connects

Table 1 Crystallographic and structural data for MSF–6 to MSF–9

Compound reference	MSF–6	MSF–7	MSF–8	MSF–9
Chemical formula	$C_{10}H_{14}CuIS_2$	$C_{60}H_{84}Cu_{12}I_{12}S_{12}$	$C_{38}H_{49}Cu_2I_2NOS_4$	$C_{27}H_{39}Cu_4I_4O_3S_3$
Formula Mass	388.77	3475.27	1044.90	1269.60
Crystal system	Monoclinic	Triclinic	Monoclinic	Trigonal
Space group	*C*2/*m*	$P\bar{1}$	*C*2/*c*	$R\bar{3}c$
a/Å	8.792(5)	11.1804(9)	24.998(6)	16.6650(5)
b/Å	21.509(12)	17.396(1)	8.734(2)	16.6650(5)
c/Å	7.436(4)	25.706(2)	22.402(6)	57.781(8)
α/°	90.00	107.456(1)	90.00	90.00
β/°	103.882(7)	90.016(2)	101.507(2)	90.00
γ/°	90.00	95.251(1)	90.00	120.00
Unit cell volume/Å^3	1365.1(13)	4747.2(7)	4793(2)	13897(2)
Temperature/K	291(2)	291(2)	291(2)	291(2)
No. of formula units per unit cell, *Z*	4	2	4	12
Absorption coefficient, *μ*/mm^{-1}	4.131	6.827	2.376	4.628
No. of reflections measured	3714	26254	12340	24250
No. of independent reflections	1386	18334	4689	3050
R_{int}	0.0462	0.0216	0.0379	0.0929
Final R_1 values ($I > 2\sigma(I)$)[a]	0.0516	0.0597	0.0492	0.0481
Final $wR(F^2)$ values ($I > 2\sigma(I)$)[a]	0.1233	0.1428	0.1013	0.1161
Final R_1 values (all data)[a]	0.0649	0.0804	0.0701	0.0775
Final $wR(F^2)$ values (all data)[a]	0.1266	0.1489	0.1047	0.1226
Goodness of fit on F^2	1.050	1.023	1.081	1.005
largest diff. peak and hole (e Å^{-3})	1.012/−1.903	0.720/−1.821	0.870/−0.987	0.748/−1.118

[a] $R_1 = \Sigma||F_o| - |F_c||/\Sigma|F_o|$, $wR = [\Sigma w(F_o^2 - F_c^2)^2/\Sigma w(F_o^2)^2]^{1/2}$.

Table 2 Selected bond lengths (Å) and angles (deg) for MSF–6 to MSF–9[a]

MSF–6							
Cu1–S1	2.340(2)	Cu1–I1	2.639(1)	Cu1–Cu1^{ii}	2.833(3)	S1^{i}–Cu1–I1	103.27(6)
S1^{i}–Cu1–S1	105.8(1)	S1–Cu1–I1	114.72(6)	I1–Cu1–I1^{ii}	115.06(6)		
MSF–7							
Cu1–S7^{iii}	2.311(2)	Cu1–Cu2	2.8790(16)	Cu2–Cu4	2.8314(16)	Cu3–I1	2.7631(13)
Cu1–I4	2.6530(13)	Cu2–S3	2.345(3)	Cu3–S2	2.316(3)	Cu4–S4	2.316(3)
Cu1–I1	2.6791(13)	Cu2–I2	2.6522(13)	Cu3–I3	2.6469(13)	Cu4–I2	2.6373(13)
Cu1–I2	2.7238(14)	Cu2–I1	2.6585(14)	Cu3–I4	2.6897(13)	Cu4–I4	2.6878(14)
Cu1–Cu3	2.7834(16)	Cu2–I3	2.6873(13)	Cu3–Cu4	2.7205(17)	Cu4–I3	2.7050(13)
Cu1–Cu4	2.8608(16)	Cu2–Cu3	2.8099(17)				
S7^{iii}–Cu1–I4	109.50(7)	S3–Cu2–I2	106.23(8)	S2–Cu3–I3	115.56(7)	S4–Cu4–I2	116.69(8)
S7^{iii}–Cu1–I1	107.91(7)	S3–Cu2–I1	108.65(8)	S2–Cu3–I4	105.33(7)	S4–Cu4–I4	106.29(9)
I4–Cu1–I1	114.71(5)	I2–Cu2–I1	110.93(4)	I3–Cu3–I4	114.89(5)	I2–Cu4–I4	110.01(4)
S7^{iii}–Cu1–I2	107.95(7)	S3–Cu2–I3	108.92(8)	S2–Cu3–I1	99.72(7)	S4–Cu4–I3	100.13(8)
I4–Cu1–I2	108.45(4)	I2–Cu2–I3	110.51(4)	I3–Cu3–I1	109.44(4)	I2–Cu4–I3	110.41(4)
I1–Cu1–I2	108.14(4)	I1–Cu2–I3	111.43(5)	I4–Cu3–I1	110.84(4)	I4–Cu4–I3	113.05(5)
MSF–8							
Cu1–S1	2.329(1)	Cu1–I1	2.6389(8)	Cu1–I1^{i}	2.6761(9)	Cu1–Cu1^{i}	2.836(1)
Cu1–S2	2.358(2)						
S1–Cu1–S2	116.05(6)	S2–Cu1–I1	108.67(5)	S2–Cu1–I1^{i}	101.81(5)	I1–Cu1–I1^{i}	115.50(3)
S1–Cu1–I1	110.57(5)	S1–Cu1–I1^{i}	104.15(4)				
MSF–9							
Cu1–S1	2.280(2)	Cu1–I2	2.702(1)	Cu1–Cu2	2.725(2)	Cu2–Cu1^{i}	2.724(2)
Cu1–I1	2.607(1)	Cu2–I1	2.6772(7)	Cu1–Cu1^{i}	2.755(2)	Cu2–O1W	2.195(8)
Cu1–I1^{ii}	2.712(1)						
S1–Cu1–I1	110.67(7)	I1–Cu1–I2	113.22(4)	I2–Cu1–I1^{i}	109.91(4)	I1^{ii}–Cu2–I1	111.92(3)
S1–Cu1–I2	107.26(7)	I1–Cu1–I1^{i}	113.03(4)	S1–Cu1–I1^{i}	102.04(6)	O1W–Cu2–I1^{i}	106.89(3)

[a] Symmetry transformations: for MSF–6: (i) $-x, y, 1-z$; (ii) $-x, 1-y, 1-z$; for MSF–7: (i) $-x, -y, 1-z$; (ii) $-x, 1-y, 2-z$; (iii) $2-x, -y, 1-z$; (iv) $2-x, 1-y, 2-z$; for MSF–8: (i) $1-x, 1-y, 1-z$; for MSF–9: (i) $2-x+y, 1-x, z$; (ii) $1-y, -1+x-y, z$.

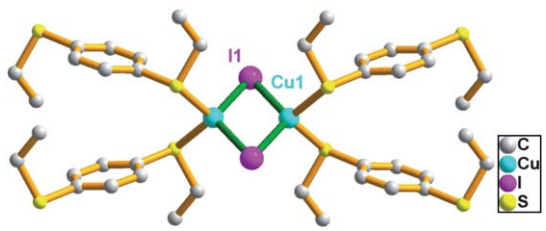

Fig. 1 A perspective drawing of the SBU in MSF–6. The H atoms are omitted for clarity.

with four thioether ligands L_1. This gives rise to a (4,4)-connecting 2D quadrangle grid sheet with **sql**/Shubnikov topology (Fig. 4). Different to that of MSF–6, which has a single lozenge grid sheet, a pair of the undulated quadrangle grid nets in MSF–7 interweave together, with adjacent rows of vertices lying on two sides of the second net-plane, to form a 2-fold interpenetrating sheet. The double sheets pack over each other in an AAA manner along the b-axis to form a 3D van der Waals network.

The structural topology of MSF–7 is the same as Cu_4I_4-(μ-$PhS(CH_2)_4SPh)_2$].[8a] Both are built upon by Cu_4I_4 cubane-like clusters as SBUs, which are interconnected *via* bridging bidentate thioether ligands to form an interpenetrated 2D coordination framework. Their differences are in that the quadrangle grid sheets in MSF–7 are highly distorted because of the rigidity of the L_1 ligand.

Structural analysis of MSF–8. MSF–8 is built from a copper-iodine cluster Cu_2I_2 unit and the linear thioether ligand L_2 (Fig. 5). The compound crystallizes in the centrosymmetric space group $C2/c$, which is associated with the point group C_{2h}. The asymmetric unit consists of one Cu, one I, one L_2 ligand, a half acetonitrile and a half guest water molecule (Fig. S2, ESI†). The Cu–I, Cu–S and Cu···Cu lengths range from 2.6389(8) to 2.6761(9) Å, 2.329(1)–2.358(2) Å and 2.836(1) Å, comparable to those reported for MSF–6, MSF–7 and other similar complexes.[5,6,16]

The structure of MSF–8 is a 2D sheet with **sql**/Shubnikov topology (Fig. 6), constructed from a 4-connecting Cu_2I_2 unit and a linear thioether linker L_2. The sheets are stacked with an ABAB sequence. The structural topology of MSF–8 is the same as MSF–6. Both complexes are built from Cu_2I_2 units and linear dithioether linkers. However, the ligand L_2 in MSF–8 is longer than that in MSF–6, which results in an undulated lozenge grid in MSF–8. The 2D sheets are stacked with an ABAB sequence, leading to free voids between the sheets in MSF–8. Inside the voids are located acetonitrile and water solvent molecules.

Structural analysis of MSF–9. X-ray single crystal diffraction analyses revealed that MSF–9 crystallizes in the centrosymmetric space group $R\bar{3}c$, which is associated with the point group D_{3d}. The compound is built from a cubane cluster Cu_4I_4 unit and the linear thioether ligand L_2 (Fig. 7). The asymmetric unit consists of one-third Cu_4I_4 cluster, a half L_2 ligand, one-third coordinated water molecule and two water guest molecules (deduced from elemental and TG analyses) (Fig. S2, ESI†). The interatomic lengths of 2.607(2) to 2.712(1) Å for Cu–I, 2.280(2) Å for Cu–S and 2.724(2) to 2.755(2) Å for Cu···Cu are in normal range. The bond valence sum calculations[15] for Cu (0.85–1.01) suggest that Cu is monovalent and there exists significant Cu···Cu interactions in the cubane-type Cu–I clusters. It is worth mentioning that each cubane cluster connects *via* its Cu atoms to three L_2 ligands, with the forth Cu to a terminal water molecule.

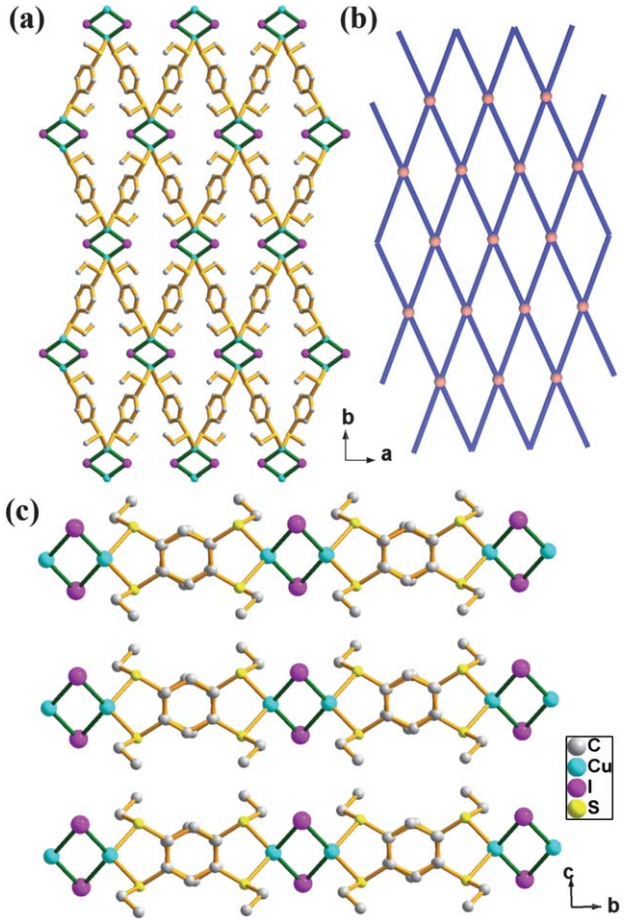

Fig. 2 Balls-and-sticks (a) and topological (b) representations of a 2D layer and (c) packing view of MSF–6. The H atoms are omitted for clarity.

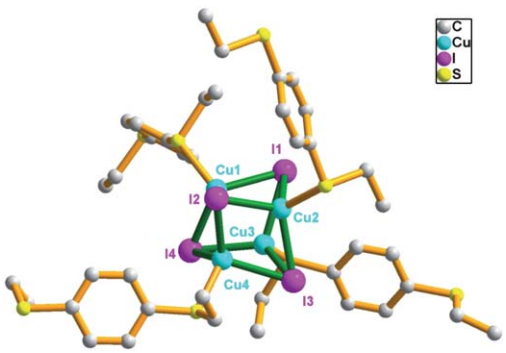

Fig. 3 A perspective drawing of the SBU in MSF–7. The H atoms are omitted for clarity.

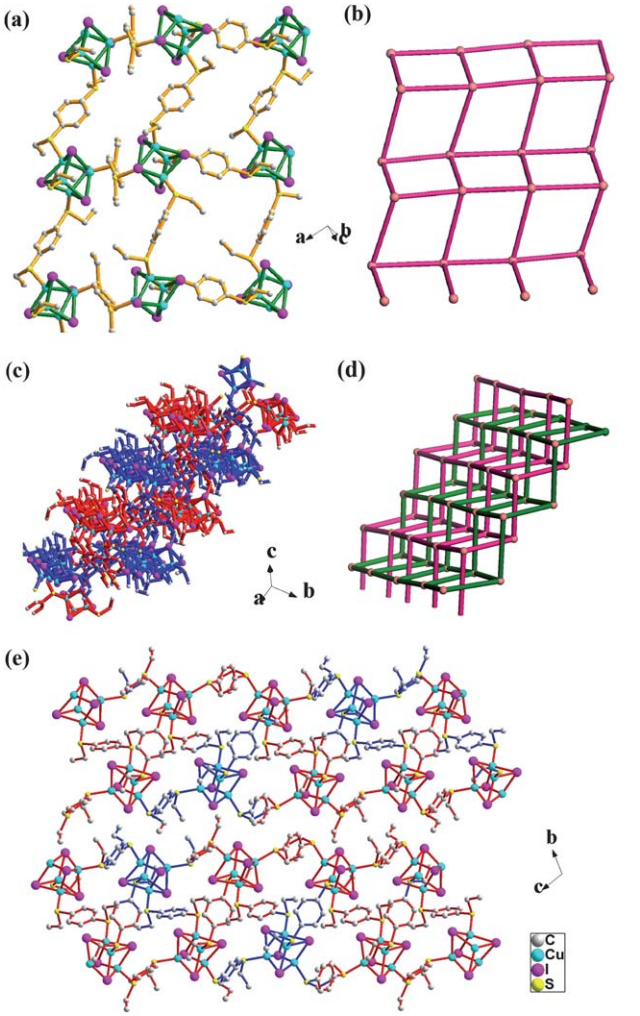

Fig. 4 Balls-and-sticks (a, c) and topological (b, d) representations of a single and 2-fold interpenetrating layers in MSF–7. (e) Packing view of MSF–7. The H atoms are omitted for clarity.

Fig. 5 A perspective drawing of the SBU in MSF–8. The H atoms are omitted for clarity.

The framework of MSF–9 is constructed from a 3-connecting Cu_4I_4 units, and a linear thioether linker L_2 (Fig. 8). This gives rise to a 2D honeycomb sheet with **hcb** topology (point symbol 6^3), in which Cu_4I_4 clusters define the corners and the dithioether ligands the edges. Three adjacent **hcb** sheets interpenetrate with each other, leading to a 3-fold interpenetration 2D layer with the coordination water molecules pointing outside of the layer. The layers stack over each other in an ABC manner along the c-axis. The coordinated terminal water molecules on Cu_4I_4 clusters in one layer protrude deeply into the pockets of adjacent layers to form a 3D van der Waals network. In comparison, MSF–7 is also formed from cubane-like Cu_4I_4 clusters and linear dithioether ligands, but with a 2-fold interpenetrating **sql** layered structure. The difference is likely due to the length of the ligands used in the construction of two compounds. The linker L_2 in MSF–9 is longer and results in larger cavities, which allow 3-fold interpenetration to stabilize the framework.

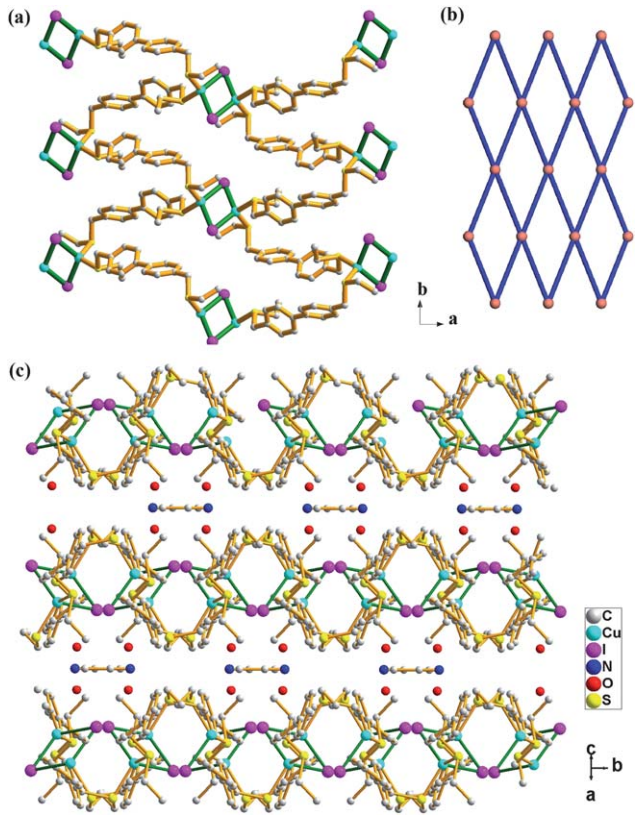

Fig. 6 Balls-and-sticks (a) and topological (b) representations of a 2D layer and (c) packing view of MSF–8. The H atoms are omitted for clarity.

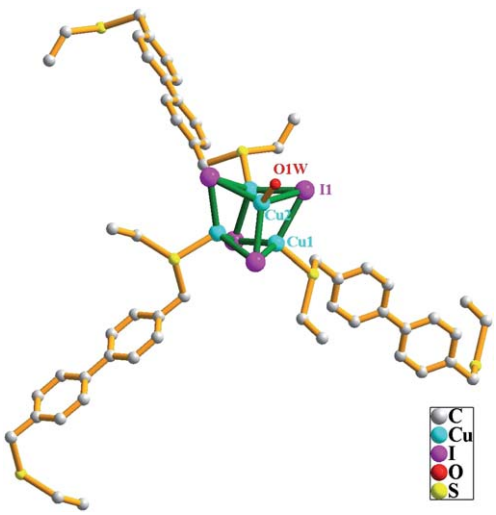

Fig. 7 A perspective drawing of the SBU in MSF–9. The H atoms are omitted for clarity.

MSF–9 has some similarities with the reported $Cu_4I_4(PhCH_2S(CH_2)_4SCH_2Ph)_{1.5}$.[8b] Both are built from cubane-like Cu_4I_4 clusters and linear dithioether ligands, which form (6,3) topological sheets. In the latter, however, the Cu_4I_4 clusters in one 2D sheet connect *via* μ^4-I with other cores in the adjacent layers to form a 3D framework.

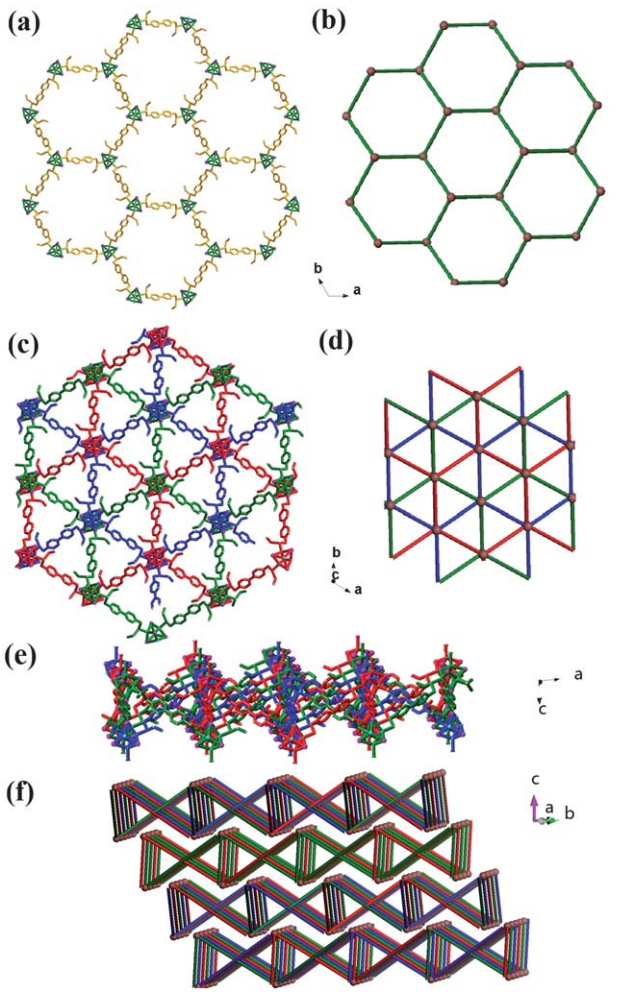

Fig. 8 Balls-and-sticks (a, c, e) and topological (b, d) representations of a single and 3-fold interpenetrating layers in MSF–9. (f) Packing view of MSF–9. The H atoms and solvent molecules are omitted for clarity.

Thermal studies

To study the thermal stability of MSF–*n* ($n = 6$–9), thermogravimetric analyses (TGA) were carried out. As shown in Fig. 9, the TGA profiles show that MSF–6 and MSF–7 exhibit similar thermal decomposition behaviors. The two compounds began to lose the ligand L_1 leaving the copper iodide portion from *ca.* 114 to 190 °C, with weight losses of 51.5% (calculated 51.0%) and 34.6% (calculated 34.2%) for MSF–6 and MSF–7, respectively. Above *ca.* 525 °C, both started to vaporize residue CuI (observed 48.7% and 62.4, calculated 49.0% and 65.8% for MSF–6 and MSF–7, respectively).

MSF–8 and MSF–9 also exhibit similar thermal decomposition behaviors. MSF–8 began to lose acetonitrile and water guest molecules from *ca.* 58 to 80 °C, with a weight loss of 3.8% (calculated 5.6%). Above *ca.* 200 °C, MSF–8 started to lose parts of its ligand L_2 ($-CH_2PhPhCH_2-$, –Et) as a result of thermal decomposition (observed 39.6%, calculated 40.1%). Above *ca.* 520 °C, the residue of MSF–8 further decomposed and vaporized. MSF–9 was stable until at *ca.* 230 °C when it started to lose the coordinated water and decompose the ligand L_2 with a weight loss of 30.6% (calculated 32.0%). Above *ca.* 580 °C, parts of the residue started to vaporize.

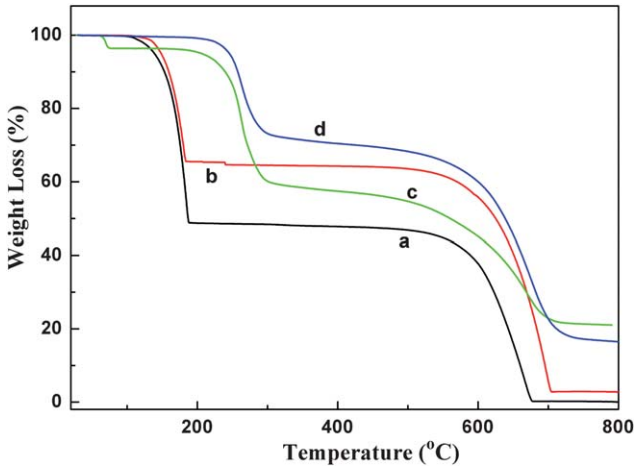

Fig. 9 TGA profiles of MSF–6(a) to MSF–9(d) under nitrogen.

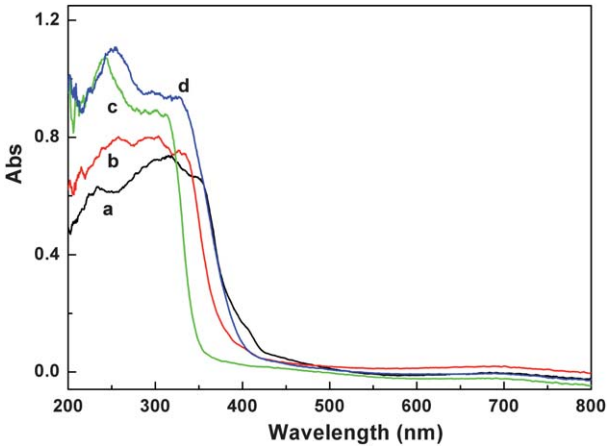

Fig. 10 The solid-state diffuse reflectance UV-Vis spectra for MSF–6 to MSF–9 (a–d).

It is noted that there are apparent differences in thermal behaviors of MSF–6 and MSF–7 with MSF–8 and MSF–9, which could be attributed to the ligand effects. Complexes MSF–6 and MSF–7 with ligand L_1 are less thermally stable than the ligand L_2-based MSF–8 and MSF–9. The former were transformed into CuI upon release of ligand L_1 at *ca.* 114 °C, while the latter turned into unknown Cu–S–I phases at *ca.* 200 °C after the decomposition of ligand L_2. Upon heating at higher temperatures, most of the CuI residue in MSF–6 and MSF–7 vaporized, while the Cu–S–I in MSF–8 and MSF–9 only partially decomposed.

The solid state UV-Vis spectra

Considering that chalcogenide materials are usually semiconducting, we studied the semiconducting properties of MSF–6 to MSF–9. The band-gap energies in semiconducting materials can be evaluated directly from the absorption spectrum.[17] The solid state diffuse-reflectance UV-Vis spectra using $BaSO_4$ powder as a 100% reflectance reference were recorded, which show that the compounds have an absorption onset at about 400, 383, 353 and 405 nm for MSF–6 to MSF–9, respectively (Fig. 10). The results indicate that MSF–6 to MSF–9 are wide-gap semiconductors with band gaps of 3.11 (MSF–6), 3.25 (MSF–7), 3.52 (MSF–8) and 3.07 (MSF–9) eV, respectively. These band gaps are comparable to those of the reported sulfide frameworks of CMF–2 ($[Cd_{17}S_4(SC_6H_4Me\text{-}4)_{28}]^{2-}$, 2.99 eV),[18] CMF–4 ($[Cd_{17}S_4(SPhMe\text{-}3)_{28}]^{2-}$, 2.88 eV),[19] and MSF–5 ($[Cd_{17}S_4(SPhMe\text{-}4)_{27}(SH)]^{2-}$, 3.14 eV).[10c]

Photoluminescent properties

The photoluminescent properties of MSF–6 to MSF–9 in the solid state were studied at room temperature. Both Cu_4I_4 cubane cluster-based coordination polymers MSF–7 and MSF–9 showed photoluminescence, while Cu_2I_2-based MSF–6 and MSF–8 did not emit at room temperature upon excitation. As shown in Fig. 11, MSF–7 showed a broad yellow photoluminescence with an emission maximum at 560 nm at room temperature upon excitation at 360 nm, while MSF–9 exhibited very weak, broad emissions with an emission maximum at *ca.* 530 nm. The emissions of MSF–7 and MSF–9 can be attributed to a triplet "cluster-centered" (^{3}CC*) excited-state with mixed halide-to-metal charge-transfer (^{3}XMCT*) and "metal cluster centered" (^{3}MCC*) $d_{Cu} \rightarrow (s,p)_{Cu}$ transitions, as observed in many Cu_4I_4 cluster-based complexes.[5–7,20,21] The existence of a ^{3}MCC* contribution is supported by the closest Cu···Cu non-bonding interactions of 2.720(2) and 2.724(2) Å in MSF–7 and MSF–9, respectively, shorter than the sum of the van der Waals radii (2.80 Å).

In Cu_2I_2-based complexes MSF–6 and MSF–8, on the other hand, the Cu···Cu distances are longer than the sum of the van der Waals radii (2.80 Å), preventing observation of the ^{3}CC* emission band in the low energy region. The absence of emission bands in the high energy region in MSF–6 and –8 is probably due to luminescence quenching through the exciton transfer between the two separate π electronic systems, similar to those of the Cu(I) iodide complexes containing *para*-substituted *trans*-stibazolic ligands.[22] In those complexes, the extension of π-conjugation of the *trans*-stibazolic ligands leads to emission quenching as a result of the mixing of HOMO and LUMO orbitals when

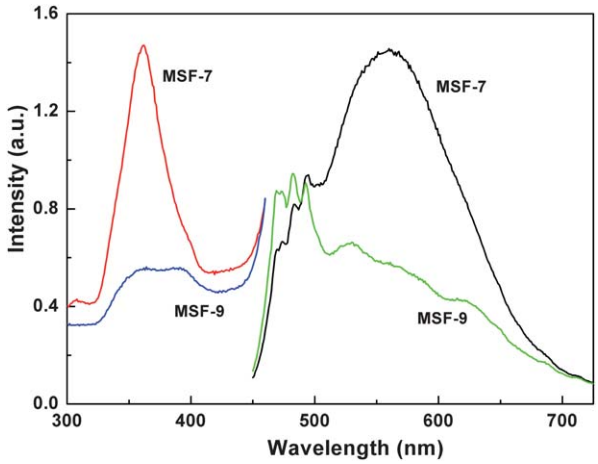

Fig. 11 Excitation (left) and emission spectra (right, excited at 360 nm for MSF–7 and 375 nm for MSF–9) of MSF–7 and MSF–9 at room temperature.

intermolecular distances are shorter than 7 Å. Relatively short intermolecular distances of 4.39 (MSF–6) and 5.24 (MSF–8) Å (measured from centre to centre between adjacent phenyl rings) were indeed found in both compounds by careful examination on their crystal structures.

Conclusions

By using linear dithioether linkers 1,4-bis(ethylthio)benzene (L_1) and 4,4′-bis(ethylthiomethyl)biphenyl (L_2), we have successfully synthesized four new coordination polymers $(CuI)_x(L)_y \cdot z$-(solvent), MSF–*n* (**m**etal-**s**ulfide-**f**ramework, MSF–6, $x = y = 2$, $L = L_1$; MSF–7, $x = 4$, $y = 2$, $L = L_1$; MSF–8, $x = y = 2$, $L = L_2$; MSF–9, $x = 4$, $y = 1.5$, $L = L_2$). The formations of these four complexes are very much dependent on the metal-to-iodine ratios and the ligands used during the synthesis. These materials exhibit interesting structural topologies, thermal behaviors and photoluminescent properties. The preparations of MSF–*n* ($n = 6$–9) imply more S-donor based coordination polymers to be forthcoming.

Acknowledgements

We are grateful for financial support from the National Basic Research Program (2011CB808704 and 2007CB925101), and the National Natural Science Foundation of China (21021062 and 20931004).

Notes and references

1 (*a*) H. Li, M. Eddaoudi, M. O'Keeffe and O. M. Yaghi, *Nature*, 1999, **402**, 276; (*b*) S. Kitagawa and M. Kondo, *Bull. Chem. Soc. Jpn.*, 1998, **71**, 1739; (*c*) J. R. Long and O. M. Yaghi, *Chem. Soc. Rev.*, 2009, **38**, 1213.

2 (*a*) M. O'Keeffe, M. Eddaoudi, H. Li, T. Reineke and O. M. Yaghi, *J. Solid State Chem.*, 2000, **152**, 3; (*b*) G. Ferey, *J. Solid State Chem.*, 2000, **152**, 37; (*c*) O. M. Yaghi, M. O'Keeffe, N. W. Ockwig, H. K. Chae, M. Eddaoudi and J. Kim, *Nature*, 2003, **423**, 705; (*d*) D. J. Tranchemontagne, Z. Ni, M. O'Keeffe and O. M. Yaghi, *Angew. Chem., Int. Ed.*, 2008, **47**, 5136.

3 (*a*) T. Devic, C. Serre, N. Audebrand, J. Marrot and G. Ferey, *J. Am. Chem. Soc.*, 2005, **127**, 12788; (*b*) Y. Qiu, H. Deng, S. Yang, J. Mou, C. Daiguebonne, N. Kerbellec, O. Guillou and S. R. Batten, *Inorg. Chem.*, 2009, **48**, 3976; (*c*) T. Murase, K. Otsuka and M. Fujita, *J. Am. Chem. Soc.*, 2010, **132**, 7864; (*d*) N. Masciocchi, S. Galli, V. Colombo, A. Maspero, G. Palmisano, B. Seyyedi, C. Lamberti and S. Bordiga, *J. Am. Chem. Soc.*, 2010, **132**, 7902; (*e*) P. E. Ryan, C. Lescop, D. Laliberte, T. Hamilton, T. Maris and J. D. Wuest, *Inorg. Chem.*, 2009, **48**, 2793.

4 S.-T. Zheng, J. Zhang and G.-Y. Yang, *Angew. Chem., Int. Ed.*, 2008, **47**, 3909.

5 (*a*) J.-K. Cheng, Y.-G. Yao, J. Zhang, Z.-J. Li, Z.-W. Cai, X.-Y. Zhang, Z.-N. Chen, Y.-B. Chen, Y. Kang, Y.-Y. Qin and Y.-H. Wen, *J. Am. Chem. Soc.*, 2004, **126**, 7796; (*b*) Y. Chen, Z.-O. Wang, Z.-G. Ren, H.-X. Li, D.-X. Li, D. Liu, Y. Zhang and J.-P. Lang, *Cryst. Growth Des.*, 2009, **9**, 4963; (*c*) A. J. Blake, N. R. Brooks, N. R. Champness, M. Crew, A. Deveson, D. Fenske, D. H. Gregory, L. R. Hanton, P. Hubberstey and M. Schroder, *Chem. Commun.*, 2001, 1432.

6 (*a*) S.-B. Ren, L. Zhou, J. Zhang, Y.-Z. Li, H.-B. Du and X.-Z. You, *CrystEngComm*, 2009, **11**, 1834; (*b*) S. Hu and M. L. Tong, *Dalton Trans.*, 2005, 1165.

7 (*a*) E. Cariati, D. Roberto, R. Ugo, P. C. Ford, S. Galli and A. Sironi, *Inorg. Chem.*, 2005, **44**, 4077; (*b*) A. Vogler and H. Kunkely, *J. Am. Chem. Soc.*, 1986, **108**, 7211.

8 (*a*) M. Knorr, F. Guyon, A. Khatyr, C. Daschlein, C. Strohmann, S. M. Aly, A. S. Abd-El-Aziz, D. Fortin and P. D. Harvey, *Dalton Trans.*, 2009, 948; (*b*) C. Xie, L. Zhou, W. Feng, J. Wang and W. Chen, *J. Mol. Struct.*, 2009, **921**, 132; (*c*) S. Q. Liu, H. Konaka, T. Kuroda-Sowa, Y. Suenaga, H. Ito, G. L. Ning and M. Munakata, *Inorg. Chim. Acta*, 2004, **357**, 3621.

9 (*a*) T. H. Kim, Y. W. Shin, J. H. Jung, J. S. Kim and J. Kim, *Angew. Chem., Int. Ed.*, 2008, **47**, 685; (*b*) H. N. Peindy, F. Guyon, A. Khatyr, M. Knorr and C. Strohmann, *Eur. J. Inorg. Chem.*, 2007, 1823; (*c*) M. Heller and W. S. Sheldrick, *Z. Anorg. Allg. Chem.*, 2004, **630**, 1869; (*d*) T. H. Kim, K. Y. Lee, Y. W. Shin, S.-T. Moon, K.-M. Park, J. S. Kim, Y. Kang, S. S. Lee and J. Kim, *Inorg. Chem. Commun.*, 2005, **8**, 27; (*e*) J. Y. Lee, S. Y. Lee, W. Sim, K.-M. Park, J. Kim and S. S. Lee, *J. Am. Chem. Soc.*, 2008, **130**, 6902.

10 (*a*) X.-L. Yang, S.-B. Ren, J. Zhang, Y.-Z. Li, H.-B. Du and X.-Z. You, *J. Coord. Chem.*, 2009, **62**, 3782; (*b*) X.-L. Yang, J. Zhang, S.-B. Ren, Y.-Z. Li, H.-B. Du and X.-Z. You, *Inorg. Chem. Commun.*, 2010, **13**, 546; (*c*) X.-L. Yang, J. Zhang, S.-B. Ren, Y.-Z. Li, W. Huang, H.-B. Du and X.-Z. You, *Inorg. Chem. Commun.*, 2010, **13**, 1337; (*d*) J. Zhang, Y.-S. Xue, L.-L. Liang, S.-B. Ren, Y.-Z. Li, H.-B. Du and X.-Z. You, *Inorg. Chem.*, 2010, **49**, 7685.

11 L. Testaferri, M. Tingoli and M. Tiecco, *J. Org. Chem.*, 1980, **45**, 4376.

12 *SMART, and SADABS*, Bruker AXS Inc., Madison, Wisconsin, USA.

13 G. M. Sheldrick, *Acta Crystallogr., Sect. A: Found. Crystallogr.*, 2008, **64**, 112.

14 (*a*) A. L. Spek, *J. Appl. Crystallogr.*, 2003, **36**, 7; (*b*) A. L. Spek, *PLATON, A Multipurpose Crystallographic Tool*, Utrecht University, The Netherlands, 2006.

15 I. D. Brown and D. Altermatt, *Acta Crystallogr., Sect. B: Struct. Sci.*, 1985, **41**, 244.

16 (*a*) B. Kure, S. Ogo, D. Inoki, H. Nakai, K. Isobe and S. Fukuzumi, *J. Am. Chem. Soc.*, 2005, **127**, 14366; (*b*) P. L. Caradoc-Davies, L. R. Hanton, J. M. Hodgkiss and M. D. Spicer, *J. Chem. Soc., Dalton Trans.*, 2002, 1581; (*c*) R. D. Adams, M. Huang and S. Johnson, *Polyhedron*, 1998, **17**, 2775.

17 W. Z. Shen, *Int. J. Infrared Millimeter Waves*, 2002, **23**, 61.

18 Q. Zhang, X. Bu, J. Zhang, T. Wu and P. Feng, *J. Am. Chem. Soc.*, 2007, **129**, 8412.

19 Q. Zhang, Y. Liu, X. Bu, T. Wu and P. Feng, *Angew. Chem., Int. Ed.*, 2008, **47**, 113.

20 P. C. Ford, E. Cariati and J. Bourassa, *Chem. Rev.*, 1999, **99**, 3625.

21 (*a*) M. Vitale and P. C. Ford, *Coord. Chem. Rev.*, 2001, **219–221**, 3; (*b*) V. W.-W. Yam and K. K.-W. Lo, *Chem. Soc. Rev.*, 1999, **28**, 323.

22 E. Cariati, D. Roberto, R. Ugo, P. C. Ford, S. Galli and A. Sironi, *Inorg. Chem.*, 2005, **44**, 4077.